

# Hemispherically lateralized rhythmic oscillations in the cingulate-amygda circuit drive affective empathy in mice

## Highlights

- The lateralized rACC-rBLA circuit is responsible for observational fear (OF)
- 5–7 Hz oscillations in rACC and rBLA increase during OF
- 5–7 Hz oscillations in rACC and rBLA are causally involved in OF
- Hippocampal type-2 theta bi-directionally modulates the ACC-BLA theta and OF

## Authors

Seong-Wook Kim, Minsoo Kim,  
Jinhee Baek, ..., Duk-Soo Kim,  
Jin Hyung Lee, Hee-Sup Shin

## Correspondence

shin@ibs.re.kr

## In brief

Kim et al. report that the hippocampus-dependent 5–7 Hz oscillations in the cingulo-amygda circuit in the right hemisphere are specifically required for expression of empathic fear in mice. They demonstrate a causal relationship between this rhythm and empathic fear.



## Article

# Hemispherically lateralized rhythmic oscillations in the cingulate-amamygdala circuit drive affective empathy in mice

Seong-Wook Kim,<sup>1,9</sup> Minsoo Kim,<sup>1,2,9</sup> Jinhee Baek,<sup>1,9</sup> Charles-Francois Latchoumane,<sup>1</sup> Gireesh Gangadharan,<sup>3</sup> Yongwoo Yoon,<sup>1</sup> Duk-Soo Kim,<sup>4</sup> Jin Hyung Lee,<sup>2,5,6,7</sup> and Hee-Sup Shin<sup>1,8,10,\*</sup>

<sup>1</sup>Center for Cognition and Sociality, Institute for Basic Science (IBS), Daejeon 34126, Republic of Korea

<sup>2</sup>Department of Neurology and Neurological Sciences, Stanford University, Stanford, CA 94305, USA

<sup>3</sup>Department of Cell and Molecular Biology, Manipal School of Life Sciences, Manipal Academy of Higher Education, Manipal 576104, Karnataka, India

<sup>4</sup>Department of Anatomy, College of Medicine, Soonchunhyang University, Cheonan-Si 31151, Republic of Korea

<sup>5</sup>Department of Bioengineering, Stanford University, Stanford, CA 94305, USA

<sup>6</sup>Department of Neurosurgery, Stanford University, Stanford, CA 94305, USA

<sup>7</sup>Department of Electrical Engineering, Stanford University, Stanford, CA 94305, USA

<sup>8</sup>SL Bigen, Incheon 21983, Republic of Korea

<sup>9</sup>These authors contributed equally

<sup>10</sup>Lead contact

\*Correspondence: shin@ibs.re.kr

<https://doi.org/10.1016/j.neuron.2022.11.001>

## SUMMARY

Observational fear, a form of emotional contagion, is thought to be a basic form of affective empathy. However, the neural process engaged at the specific moment when socially acquired information provokes an emotional response remains elusive. Here, we show that reciprocal projections between the anterior cingulate cortex (ACC) and basolateral amygdala (BLA) in the right hemisphere are essential for observational fear, and 5–7 Hz neural oscillations were selectively increased in those areas at the onset of observational freezing. A closed-loop disruption demonstrated the causal relationship between 5–7 Hz oscillations in the cingulo-amamygdala circuit and observational fear responses. The increase/decrease in theta power induced by optogenetic manipulation of the hippocampal theta rhythm bi-directionally modulated observational fear. Together, these results indicate that hippocampus-dependent 5–7 Hz oscillations in the cingulo-amamygdala circuit in the right hemisphere are the essential component of the cognitive process that drives empathic fear, but not freezing, in general.

## INTRODUCTION

Humans and animals can acquire fear by observing conspecifics being subjected to aversive events, a phenomenon termed observational fear.<sup>1–4</sup> Studies in humans have demonstrated that observational fear responses are positively associated with trait empathy.<sup>5,6</sup> In observational fear learning in rodents, observing the demonstrator's distress responses can serve as a vicarious unconditional stimulus (US) that elicits a memory in the observer of the association between an affective experience and the specific environmental context (i.e., context-dependent conditioning).<sup>2,7</sup> Observing the demonstrator in distress must induce a similar affective experience in the observer. Thus, observational fear is considered an example of emotional contagion as a basic form of affective empathy.

Establishment of an observational fear learning assay in rodents has made it possible to study the neural circuits and genetic mechanisms underlying affective empathy. Two alternative observa-

tional fear assays measure animal behaviors that are driven by two similar processes, but with important differences. One assay, using naive observers, exclusively measures empathic fear responses to foot-shocks experienced by others,<sup>2,8,9</sup> whereas the second assay, using previously foot-shocked observers, predominantly measures adaptive learned responses in the experienced observer that are strongly amplified by observing others receiving similar foot-shocks.<sup>10–12</sup> Although the two assays share a similar behavioral outcome, it has now become clear that they are mediated by different neural mechanisms.<sup>12</sup> For example, the anterior cingulate cortex (ACC), which has been implicated in observational fear in both humans<sup>13</sup> and rodents,<sup>2,14,15</sup> does not affect observational fear behaviors of experienced observers.<sup>10,11</sup> Importantly, a recent study clearly showed that the observational freezing of experienced observers was in fact strongly driven by neural circuits that mediate contextual fear.<sup>12</sup> In contrast, it remains to be determined how observational fear is driven in naive observers, which more closely reflects affective empathy.



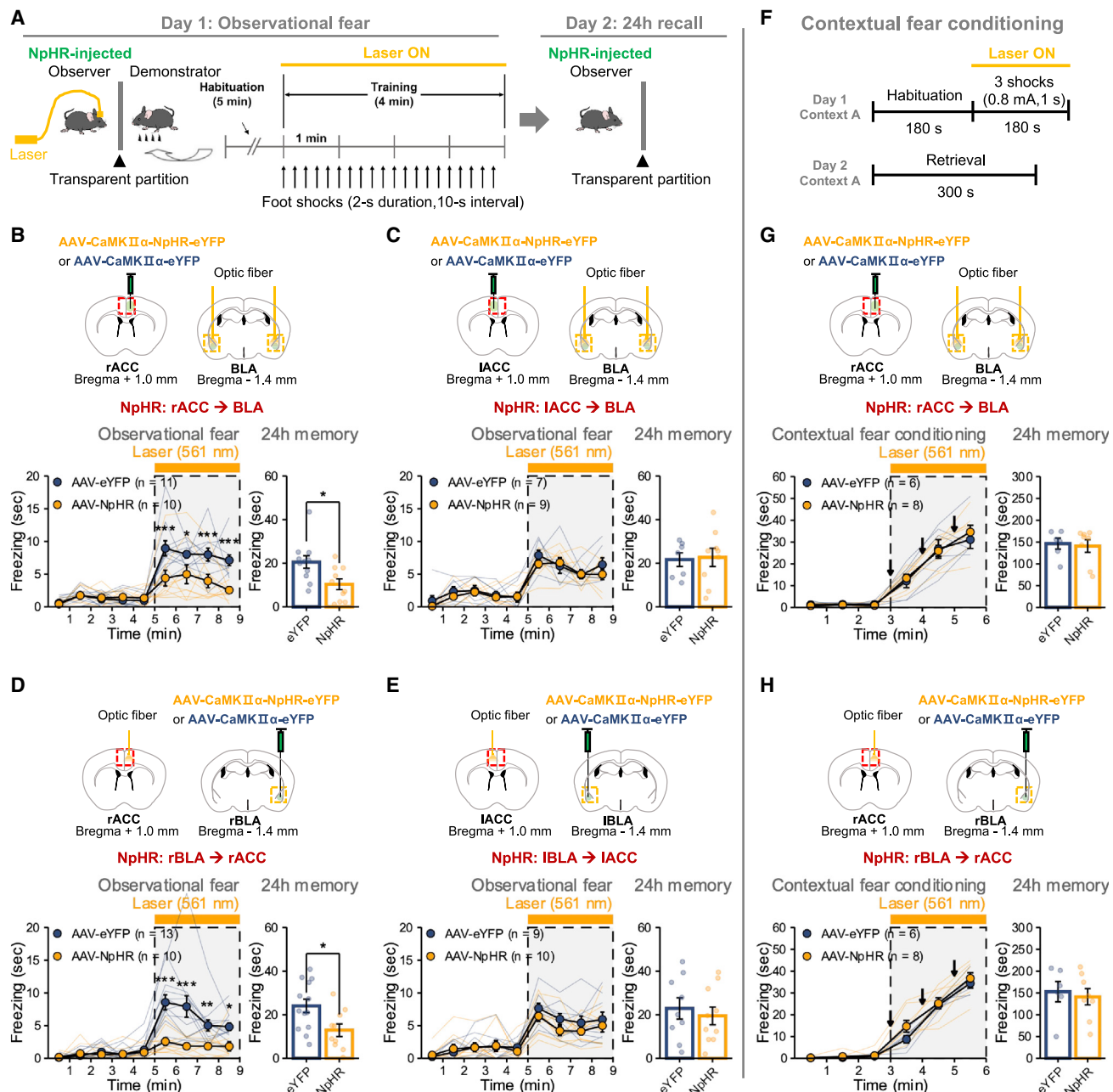


**Figure 1. Reciprocal connections between the rACC and rBLA selectively control observational fear**

- (A) Schematic illustrations of behavioral procedures for testing socially transferred fear.
- (B) AAV5-CaMKII $\alpha$ -NpHR3.0-eYFP was injected into the right ACC, and the BLA was bilaterally illuminated with a yellow laser (top). Optogenetic inhibition of rACC-BLA projections significantly reduced freezing during observational fear (bottom left;  $F_{1, 19} = 14.224$ ,  $p = 0.001$ , two-way repeated measures ANOVA) and subsequent 24-h contextual memory (bottom right;  $p < 0.05$ ,  $t(19) = -2.671$ , t test).
- (C) Optogenetic inhibition of the IACC-BLA pathway (top) did not change freezing during observational fear (bottom left;  $F_{1, 14} = 1.079$ ,  $p = 0.317$ , two-way repeated measures ANOVA) or 24-h memory recall (bottom right;  $p = 0.851$ ,  $t(14) = 0.192$ , t test).
- (D) AAV5-CaMKII $\alpha$ -NpHR3.0-eYFP was injected into the right BLA, and the right ACC was illuminated with a yellow laser (top). Optogenetic inhibition of rBLA-rACC projections significantly reduced freezing during observational fear (bottom left;  $F_{1, 21} = 12.858$ ,  $p < 0.01$ , two-way repeated measures ANOVA) and subsequent 24-h contextual memory (bottom right;  $p < 0.05$ ,  $t(21) = -2.251$ , t test).
- (E) Optogenetic inhibition of the IBLA-IACC pathway (top) did not change freezing during observational fear (bottom left;  $F_{1, 17} = 0.996$ ,  $p = 0.332$ , two-way repeated measures ANOVA) or 24-h memory recall (bottom right;  $p = 0.596$ ,  $t(17) = -0.541$ , t test).
- (F) Schematic illustrations of behavioral procedures for testing contextual fear conditioning.

(legend continued on next page)

Previous studies with naive observers have suggested the specific involvement of the ACC in the immediate, socially transferred fear, showing that it is required only for vicarious fear responses on day-1 conditioning, but not for expression of the contextual fear memory 24 h later.<sup>2</sup> Interestingly, only the right-side ACC is involved in observational fear—a case of hemispheric lateralization in the rodent.<sup>15</sup> It has also been shown that the basolateral amygdala (BLA) is essential for observational fear.<sup>2,8,9</sup> In addition, rhythmic oscillations at the theta frequency are observed in the ACC and BLA during observational fear.<sup>2</sup> These features present a temporal and spatial framework for investigating the neural mechanism underlying observational fear in the mouse.

To elucidate a neural mechanism underlying observational fear that conforms to the framework described above, we focused on the ACC-BLA circuit. We found that hippocampus-dependent 5–7 Hz theta synchronization in the reciprocal ACC-BLA circuit of the right hemisphere selectively drives vicarious observational fear in naive observer mice. Importantly, the function of this oscillation was unique to vicarious freezing and followed the temporal and spatial domains of this behavior.

## RESULTS

### Hemispherically lateralized cingulo-amygda circuit is specifically responsible for observational fear

First, we investigated the neural circuits involving the ACC and BLA within the context of hemispheric lateralization. The BLA receives ACC excitatory projections both from ipsilateral and contralateral hemispheres (Figures S1A and S1B). To test lateralization of ACC-to-BLA projections, we placed optical fibers over the BLA and selectively inhibited inputs from either the right or left ACC. Bilateral optogenetic inhibition of the right ACC (rACC)-to-BLA pathways impaired observational fear on day 1 and decreased fear memory on day 2 in naive observers (Figures 1A and 1B). However, bilateral inhibition of left ACC (lACC)-originating projections did not affect the freezing response (Figure 1C), demonstrating that ACC-to-BLA projections are functionally lateralized.

BLA neurons predominantly have unilateral projection to the ACC (Figures S1C and S1D). To further examine the functional lateralization of the BLA-to-ACC projections, we optogenetically inhibited the ipsilateral BLA projections through optic fibers placed unilaterally in the ACC during observational fear. We found that BLA-to-ACC projections were also functionally lateralized, where only the inhibition of right BLA-to-ACC projections impaired observational fear responses on day 1 and decreased fear memory on day 2 (Figures 1D and 1E). In sum, these results clearly show that reciprocal ACC-BLA interactions are functionally lateralized to the right hemisphere and are required for observational fear in naive observer mice.

We next investigated whether the involvement of these reciprocal connections is specific to socially transferred fear by silencing bilateral rACC-to-BLA projections or rBLA-to-rACC projections during contextual fear conditioning (Figure 1F). In contrast to observational fear, which was inhibited by optogenetic inhibition, freezing behaviors on both day 1 and 2 induced by direct foot-shock experiences and memory recall, respectively, were unchanged under these conditions (Figures 1G and 1H). These results suggest that the rACC-rBLA reciprocal connectivity is essential for socially transferred fear, but not for fear in general.

Prelimbic and infralimbic cortices of the medial prefrontal cortex (mPFC) are brain regions well-known for their reciprocal connections with the BL<sup>16</sup> and for regulation of the expression and storage of fear and its extinction.<sup>17,18</sup> To test whether observational fear requires projections from mPFC to BLA, we bilaterally injected the AAV-expressing halorhodopsin under the control of calcium/calmodulin-dependent protein kinases II $\alpha$  promoter (AAV5-CamKII $\alpha$ -NpHR3.0-eYFP) into the mPFC and inhibited the terminals of these excitatory neurons in the BLA during observational fear (Figure S1E). Unlike the bilateral rACC-to-BLA silencing, silencing of the mPFC-to-BLA pathway had no effect on the observational fear responses and the 24-h memory recall (Figure S2F), indicating that socially transferred fear and self-driven fear are separately controlled by devoted circuitries involving rACC and mPFC, respectively.

### 5–7 Hz oscillations are selectively increased during observational fear

Based on the observations showing the importance of ACC-BLA interactions in observational fear, we next investigated how the activities of these brain areas are coordinated. We previously reported the presence of synchronized theta oscillations in the ACC and amygdala during observational fear session.<sup>2</sup> However, this previous work did not address whether this theta activity is physiologically relevant and specific to observational fear responses. To address this issue, we bilaterally recorded theta oscillations in the left and right ACC (Figure 2A) or BLA (Figure 2D), and then compared these oscillations around freezing/immobility epochs during three stages of the behavioral assay: habituation, observational fear, and 24-h memory recall.

We found that relative theta power in the rACC increased in a manner that was temporally locked with freezing behavior during observational fear. Specifically, the proportion of spectral power at 5–7 Hz was significantly enhanced around the onset of observational freezing, compared with immobility during the habituation session, or freezing during the contextual recall of vicarious fear. Furthermore, the increase was significantly higher in magnitude in the rACC compared with that in the lACC (Figures 2B and 2C). Despite the possibility of volume conduction in local field potential (LFP) between the two areas that are in close proximity with strong interconnections, the significant differences of theta

(G) Inhibition of rACC-BLA projections (top) had no significant effect on freezing behavior during contextual fear conditioning (bottom left;  $F_{1,12} = 0.0587$ ,  $p = 0.813$ , two-way repeated measures ANOVA) or subsequent 24-h contextual memory (bottom right;  $p = 0.787$ ,  $t(12) = 0.276$ , t test).

(H) Inhibition of rBLA-rACC projections (top) had no effect on freezing behavior during contextual fear conditioning (bottom left;  $F_{1,12} = 1.398$ ,  $p = 0.260$ , two-way repeated measures ANOVA) or subsequent 24-h contextual memory (bottom right;  $p = 0.698$ ,  $t(12) = 0.398$ , t test). Data are presented as means  $\pm$  SEM (error bars). \* $p < 0.05$ , \*\* $p < 0.01$ , \*\*\* $p < 0.001$ ; post-hoc multiple comparisons with Bonferroni correction.

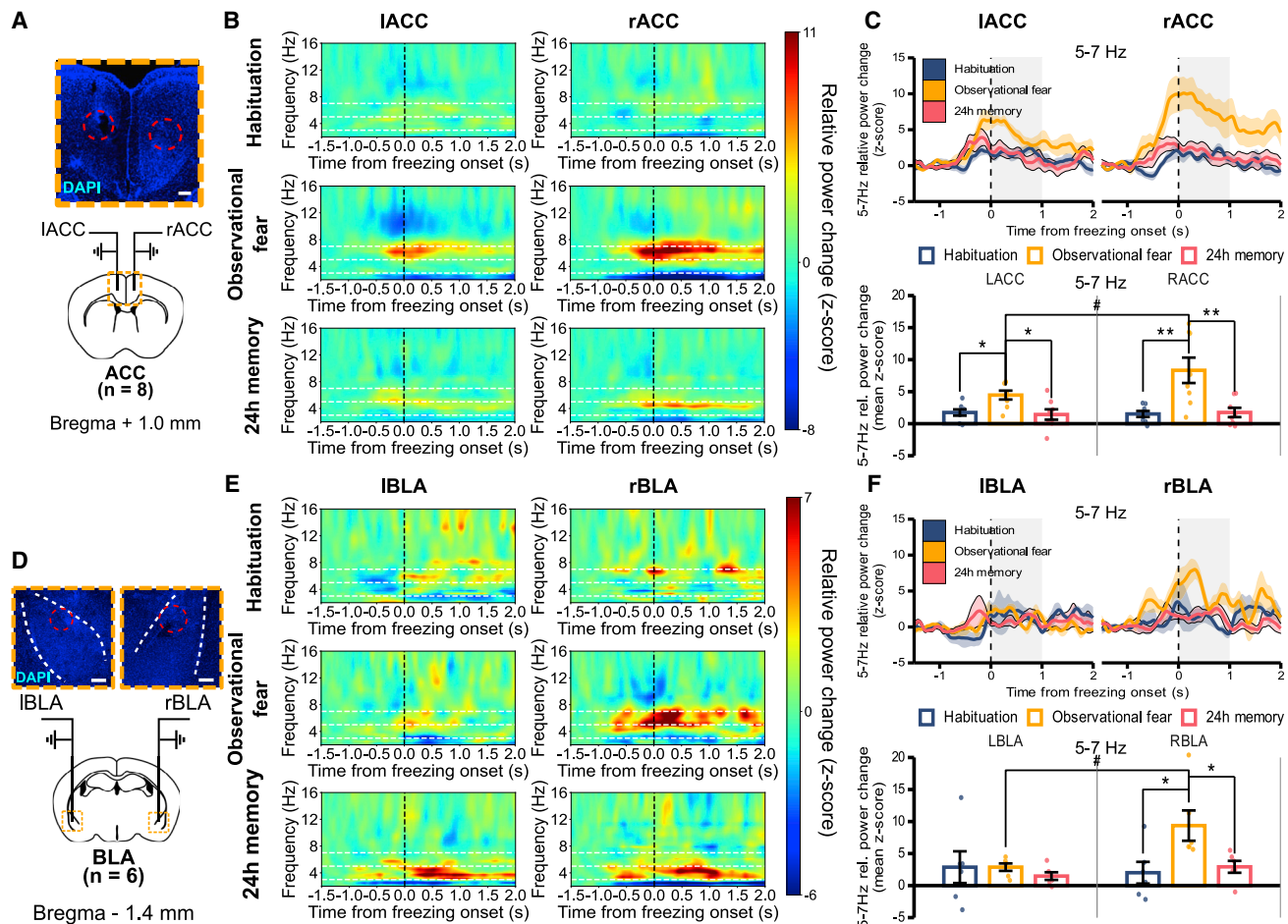


**Figure 2. 5–7 Hz theta oscillations in the ACC and BLA are selectively increased during socially transferred fear in the right hemisphere**

(A) Tetrode arrays were inserted into the left and right ACC (red circle). Scale bars, 200  $\mu$ m.

(B) Z scored relative power spectrograms recorded in the left and right ACC around the onset of immobility/freezing behavior, averaged over subjects ( $n = 8$ ). White dashes mark frequencies at 3, 5, and 7 Hz.

(C) Temporal changes in relative power at 5–7 Hz (top) and averaged Z scores from  $t = 0$  to  $t = 1$  s (bottom; IACC:  $F_{2, 14} = 6.453$ ,  $p < 0.05$ , one-way repeated measures ANOVA; rACC:  $F_{2, 14} = 9.165$ ,  $p < 0.01$ , one-way repeated measures ANOVA; IACC versus rACC: habituation,  $p = 0.7076$ ,  $t(7) = -0.3907$ , paired t test; observational fear,  $p < 0.05$ ,  $t(7) = 2.5629$ , paired t test; 24-h memory,  $p = 0.6308$ ,  $t(7) = 0.50238$ , paired t test).

(D) Tetrode arrays were inserted into the left and right BLA (red circle). Scale bars, 200  $\mu$ m.

(E) Z scored relative power spectrograms recorded in the left and right BLA around the onset of immobility/freezing behavior averaged over subjects ( $n = 6$ ). White dashes mark frequencies at 3, 5, and 7 Hz.

(F) Temporal changes in relative power at 5–7 Hz (top) and averaged Z scores from  $t = 0$  to  $t = 1$  s (bottom; IBLA:  $F_{2, 10} = 0.383$ ,  $p = 0.691$ , one-way repeated measures ANOVA; rBLA:  $F_{2, 10} = 8.204$ ,  $p < 0.01$ , one-way repeated measures ANOVA; IBLA versus rBLA: habituation,  $p = 0.429$ ,  $t(5) = -0.8601$ , paired t test; observational fear,  $p < 0.05$ ,  $t(5) = 3.1197$ , paired t test; 24-h memory,  $p = 0.08303$ ,  $t(5) = 2.1615$ , paired t test). Data are presented as means  $\pm$  SEM (shadings and error bars). \* $p < 0.05$ , \*\* $p < 0.01$ ; post-hoc multiple comparison with Bonferroni correction.

power in the simultaneously recorded signals strongly suggest that the rACC is the main area in which theta-oscillating neural processes take place during observational fear.

Similar to the rACC case, the power proportion of 5–7 Hz oscillations was selectively increased in the rBLA, temporally coinciding with the observational fear behavior (Figures 2E and 2F). The enhanced 5–7 Hz oscillations in the rACC and rBLA ended immediately as observational freezing was terminated (Figures S2A and S2B), providing further support for the strong temporal correlation between these oscillations and observational fear. Additionally, no immediate increase in 5–7 Hz oscilla-

tions was observed in the average spectrogram calculated at the demonstrator shock onset time (Figures S2C and S2D). The selective enhancement during observational freezing suggests that the increase of 5–7 Hz oscillations in the rACC and rBLA could not be accounted for by freezing in general, an increase in attention and alertness, or a decrease in mobility.

Notably, during the recall of vicarious fear on day 2, the BLA showed increased oscillations at a lower frequency range (3–5 Hz) though no significant hemispheric difference was observed (Figures 2E and 3B). This increase of oscillation around 4 Hz during fear recall is consistent with previous results reported in a

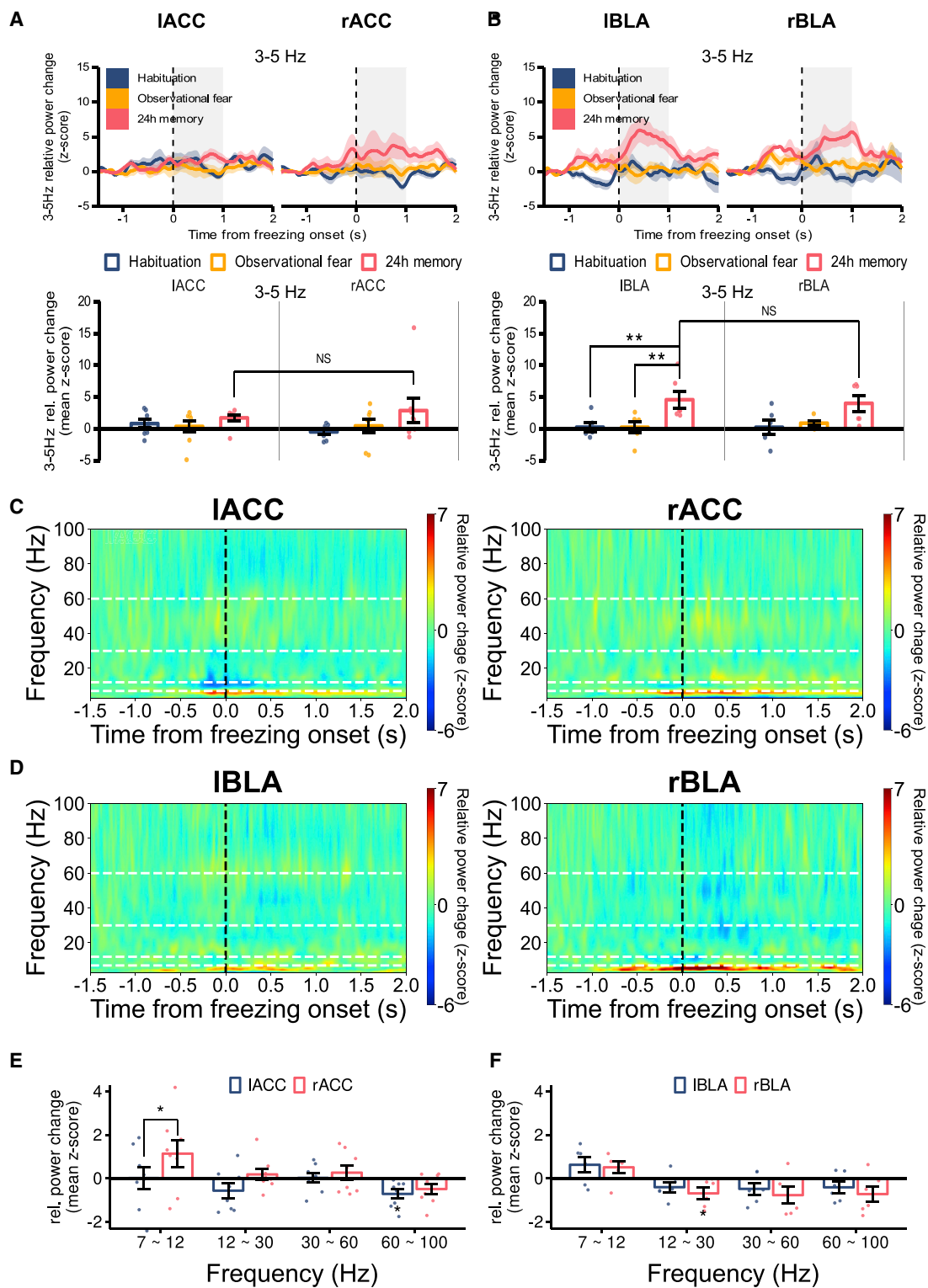


**Figure 3. Relative power changes of 3–5 Hz oscillations and higher frequency bands above 7 Hz in the ACC and the BLA around the onset of immobility/freezing**

(A) Temporal changes of the relative power in ACC at 3–5 Hz (top) and the averaged Z scores from  $t = 0$  to  $t = 1$  s (bottom; IACC:  $F_{2, 14} = 6.453$ ,  $p < 0.05$ , one-way repeated measures ANOVA; rACC:  $F_{2, 14} = 9.165$ ,  $p < 0.01$ , one-way repeated measures ANOVA; IACC versus rACC: habituation,  $p = 0.04409$ ,  $t(7) = -2.4503$ ;

(legend continued on next page)

classical fear conditioning study.<sup>19</sup> In contrast, no increase at 3–5 Hz oscillations was observed in the ACC (Figure 3A), which is consistent with the previous finding that the ACC is not involved in 24-h memory recall.<sup>2</sup> In addition, the higher frequency bands above 7 Hz did not show any significant changes in the spatial and temporal domains relevant to observational fear (Figures 3C–3F). In sum, the distinct oscillatory activity at 5–7 Hz in the rACC and rBLA during observational fear shows that observational fear is generated by previously unexplored neural oscillatory mechanisms in this neural circuit.

To further test whether the increase of 5–7 Hz oscillations in the rACC and rBLA are unique to observational fear, we recorded theta oscillations in the rACC and rBLA during the contextual fear conditioning (Figure S2E). We found that the changes of 5–7 Hz oscillations in the rACC and rBLA were not significant around the onset of freezing during intershock intervals in the contextual fear conditioning experiment (Figures S2F and S2G). For the freezing induced by the firsthand foot-shock experience, 3–5 Hz oscillations were significantly increased only in the rBLA (Figure S2G), but not in the rACC (Figure S2F). Taken together, the specific increase in 5–7 Hz oscillations in the rACC and rBLA during right hemisphere-lateralized observational fear suggests a pivotal role for these oscillations in the expression of empathic responses.

### Theta oscillations in the rACC and rBLA are causally involved in expression of observational fear

Although the current results show a close temporal and spatial relationship between 5–7 Hz theta oscillations and observational fear, whether these oscillations are essential for the empathic behavior remains unclear. To test the causal relationship between rACC theta rhythms and observational fear, we used a closed-loop manipulation to selectively disrupt theta oscillations in the rACC with minimal direct control of cell firings (Figure 4A). LFP activity in the rACC was continuously monitored during behavior, and a single, strong but brief channelrhodopsin 2 (ChR2) stimulation (5–10 mW; 10 ms), which is known to disrupt on-going brain oscillations,<sup>20,21</sup> was immediately applied whenever an increase in theta power was detected (“On-theta” in Figure 4B). As a control for ChR2 stimulation, a separate group received a delayed ChR2 stimulation in the rACC after termination of a theta epoch (“Post-theta” in Figure 4B).

Using ChR2 stimulation, we could successfully interrupt and truncate on-going theta oscillations during observational fear (Figure 4C; On-theta). In contrast, the delayed-stimulation control group showed normal theta oscillations during freezing (Figure 4C; Post-theta). 5–7 Hz relative power changes in the ACC and BLA of the On-theta group were significantly lower than those of the Post-theta group around the onset of freezing (Figure 4D). The phases of theta oscillations recorded in the rACC and rBLA were highly synchronized during observational fear in the Post-theta group (Figure 4E). This increase in phase synchrony was also disrupted by closed-loop manipulation of the rACC theta (Figure 4F), indicating the dependence of the rACC-rBLA theta synchrony on rACC oscillations. Importantly, the disruption of theta power and phase synchrony was followed by abrupt terminations of freezing behaviors initiated around theta onsets (Figure 4G). As a result, the On-theta group exhibited a significant impairment in the overall freezing behaviors during the observational fear assay, but no effect on memory of day 2 (Figure 4H).

We also applied the same closed-loop disruption in the rBLA while monitoring LFP in the rACC and rBLA (Figure S3A). Similar to the rACC manipulation in Figure 4, closed-loop ChR2 stimulation in the rBLA successfully impaired theta rhythms and their synchrony in the ACC-BLA circuit (Figures S3B–S3F), and reduced freezing during observational fear on day 1 (Figures S3G and S3H). The same ChR2 stimulation in either the ACC or the BLA, however, did not change freezing behavior when applied after termination of theta event in the Post-theta group (Figures S3I and S3J), confirming that the reduction of observational fear in the On-theta group is due to the disruption of the theta oscillations.

### Hippocampal theta bi-directionally modulates ACC-BLA theta and observational fear

The hippocampus generates theta oscillations that have been extensively studied and shown to be tightly linked with various brain functions, such as motility, memory, emotion, and spatial representation of self and others.<sup>22–26</sup> It has been suggested that hippocampal theta rhythm provides an oscillatory framework that synchronizes activities between brain areas.<sup>27–30</sup> Thus, we hypothesized that hippocampal theta waves may

observational fear,  $p = 0.9064$ ,  $t(7) = 0.1219$ ; 24-h memory,  $p = 0.5607$ ,  $t(7) = 0.61076$ , paired t test). No significant increase of the 3–5 Hz oscillations were observed during 24-h memory recall although one of the subjects showed large increase in the rACC.

(B) Temporal changes of the relative power in BLA at 3–5 Hz (top) and the averaged Z scores from  $t = 0$  to  $t = 1$  s (bottom; IBLA:  $F_{2, 10} = 0.383$ ,  $p = 0.691$ , one-way repeated measures ANOVA; rBLA:  $F_{2, 10} = 8.204$ ,  $p < 0.01$ , one-way repeated measures ANOVA; IBLA versus rBLA: habituation,  $p = 0.9891$ ,  $t(5) = -0.014299$ ; observational fear,  $p = 0.4503$ ,  $t(5) = 0.81858$ ; 24-h memory,  $p = 0.6417$ ,  $t(5) = -0.49481$ , paired t test). Shadings and error bars indicate mean  $\pm$  SEM. Post-hoc multiple comparison with Bonferroni correction: \* $p < 0.01$ .

(C and D) Z scored relative power spectrograms at 3–100 Hz in the left and right ACC (C) and BLA (D) around the onset of freezing behavior during observational fear, averaged over subjects ( $n = 8$  for the ACC, and 6 for the BLA). White dashes mark frequencies at 7, 12, 30, and 60 Hz.

(E) Relative power changes at 7–12, 12–30, 30–60, and 60–100 Hz in the left and right ACC. Averaged Z scores from  $t = 0$  to  $t = 1$  s are used for statistical analysis (IACC, one-sample t test: 7–12 Hz,  $p = 0.965$ ,  $t(7) = 0.045434$ ; 12–30 Hz,  $p = 0.1405$ ,  $t(7) = -1.6619$ ; 30–60 Hz,  $p = 0.8974$ ,  $t(7) = 0.13376$ ; 60–100 Hz,  $p = 0.01256$ ,  $t(7) = -3.3319$ ; rACC, one-sample t test: 7–12 Hz,  $p = 0.1077$ ,  $t(7) = 1.8439$ ; 12–30 Hz,  $p = 0.502$ ,  $t(7) = 0.70768$ ; 30–60 Hz,  $p = 0.4562$ ,  $t(7) = 0.78855$ ; 60–100 Hz,  $p = 0.09107$ ,  $t(7) = -1.9581$ ; IACC versus rACC,  $F_{1, 7} = 11.22$ ,  $p < 0.05$ , two-way repeated measures ANOVA).

(F) Relative power changes at 7–12, 12–30, 30–60, and 60–100 Hz in the left and right BLA. Averaged Z scores from  $t = 0$  to  $t = 1$  s were used for statistical analysis (IBLA, one-sample t test: 7–12 Hz,  $p = 0.1312$ ,  $t(5) = 1.8032$ ; 12–30 Hz,  $p = 0.1526$ ,  $t(5) = -1.6859$ ; 30–60 Hz,  $p = 0.15$ ,  $t(5) = -1.6995$ ; 60–100 Hz,  $p = 0.1922$ ,  $t(5) = -1.5067$ ; rBLA, one-sample t test: 7–12 Hz,  $p = 0.1003$ ,  $t(5) = 2.013$ ; 12–30 Hz,  $p = 0.045463$ ,  $t(5) = -2.6464$ ; 30–60 Hz,  $p = 0.09966$ ,  $t(5) = -2.0177$ ; 60–100 Hz,  $p = 0.1066$ ,  $t(5) = -1.9652$ ; IBLA versus rBLA,  $F_{1, 5} = 6.448$ ,  $p = 0.0519$ , two-way repeated measures ANOVA). Data are presented as means  $\pm$  SEM. \* $p < 0.05$ ; post-hoc multiple comparison with Bonferroni correction.

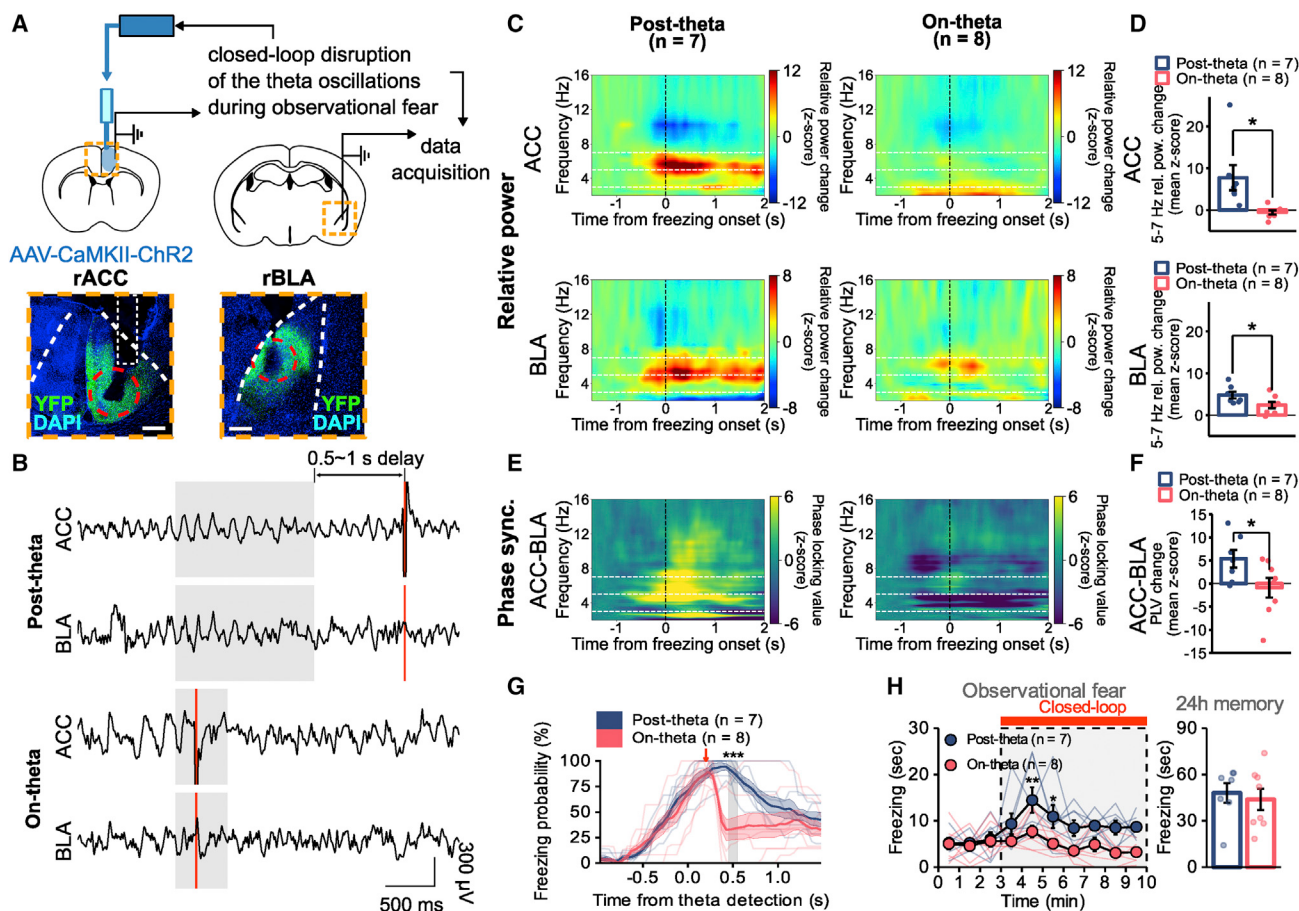


**Figure 4. Observational fear is causally dependent on rACC theta oscillations**

(A) Illustration of selective closed-loop disruption of ACC theta activity. AAV5-CaMKII $\alpha$ -ChR2-eYFP and optical fiber were targeted to the right ACC, and tetrode arrays were inserted into the ACC and BLA. Scale bars, 200  $\mu$ m.

(B) Example bandpass-filtered (1–40 Hz) LFP traces upon detection of increased ACC theta oscillations during observational fear (gray shading). A brief (10 ms), single ChR2 stimulation (red line) was applied immediately (On-theta) or randomly 0.5–1.0 s after termination of the power-increased theta (post-theta).

(C) Average Z scored power spectrograms around the onset of observational fear behaviors.

(D) Relative power changes in 5–7 Hz in the ACC and BLA. Averaged Z scores from  $t = 0$  to  $t = 1$  s are used for t test (ACC:  $p < 0.05$ ,  $t(13) = 2.9004$ ; BLA:  $p < 0.05$ ,  $t(13) = 2.1863$ , t test).

(E) Average Z scored phase-locking value around the onset of observational fear behaviors.

(F) Comparison of normalized phase-locking value from  $t = 0$  to  $t = 1$  ( $p < 0.05$ ,  $t(13) = 2.1621$ , t test).

(G) Probability of freezing around the onset of online detected theta oscillations ( $p < 0.001$ ,  $t(13) = 4.5564$ , t test; red arrow, the time of light stimulation in On-theta; gray shading, the time period used for t test, 0.45–0.55 s).

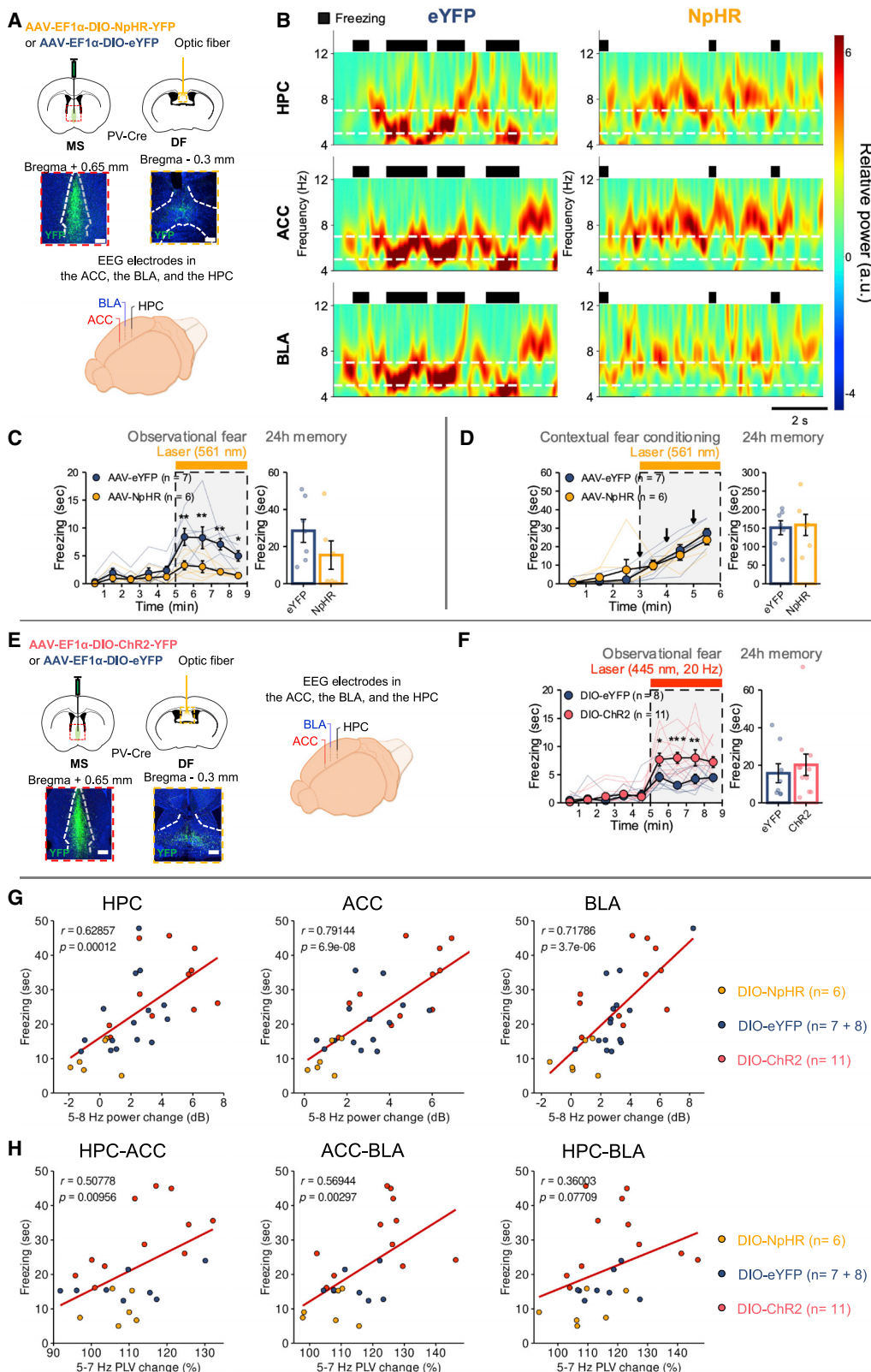
(H) Closed-loop disruption of rACC theta activity significantly reduced observational fear (left;  $F_{1,13} = 15.85$ ,  $p < 0.01$ , two-way repeated measures ANOVA). Data are presented as means  $\pm$  SEM (shadings and error bars). \*\* $p < 0.01$ ; post-hoc multiple comparison with Bonferroni correction. No significant difference for the 24-h recall between the Post-theta and On-theta groups (right;  $p = 0.6687$ ,  $t(13) = 0.43784$ , t test).

tune the synchronized theta oscillations in the rACC and rBLA during observational fear. To test this hypothesis, we selectively modulated lower range of theta in the entire hippocampal complex during observational fear assays by optogenetic manipulation of medial septum (MS)-to-hippocampal GABAergic projections at the dorsal fornix, following a previously described procedure (Figures 5A and 5B).<sup>31,32</sup>

We first investigated whether hippocampal theta rhythm is modulated during observational fear behavior in DIO-eYFP (cre-recombinase-dependent eYFP-expressing) control PV-cre (expressing cre recombinase in parvalbumin-positive neurons)

mice. All three brain areas, including the hippocampus, showed an increase in normalized power at 5–7 Hz around the onset of the observational freezing epochs (Figure S4A). Phase synchrony between the three areas was also enhanced around freezing (Figure S4B), suggesting a tight association of hippocampal theta rhythm with observational fear.

To examine the relationship between hippocampal theta and rACC and rBLA theta rhythms, we next compared the spectral power of 5–7 Hz oscillations in the three brain areas during the theta epochs identified in the rACC. The DIO-eYFP control group showed a significant increase in theta power during observational



(legend on next page)

fear sessions (Figures S4C, S4F, and S4I). However, this increase in power was impaired by optogenetic inhibition in the DIO-NpHR group (Figures S4D, S4E, S4G, S4H, S4J, and S4K), demonstrating that the enhanced theta oscillations in the rACC and rBLA are indeed hippocampus-dependent. Following the reduction in theta power, the DIO-NpHR group also showed markedly impaired observational fear behavior on day 1, but not significantly decreased freezing on day 2 (Figure 5C). The same optogenetic inhibition did neither affect contextual fear on day 1 or 2 (Figure 5D).

Finally, we examined whether enhancement of theta power further enhanced observational fear behavior. To this end, we injected DIO-ChR2 virus into the MS of PV-cre mice and applied a pulsed-light stimulation paradigm that was previously shown to increase the power of on-going type-2 hippocampal theta rhythm<sup>32</sup> (Figures 5E and S5A). We confirmed that optogenetic stimulation during observational fear enhanced 5–7 Hz theta power (Figures S5B–S5J) and led to an increase in freezing levels in the DIO-ChR2 group (Figure 5F). A detailed analysis revealed a significant positive correlation between the level of freezing and the increase in theta power in each recorded area (Figure 5G). Consistent with this, the degree of increase in phase locking value was also positively correlated with freezing behavior (Figure 5H).

Taken together, optogenetic manipulations of septo-hippocampal GABAergic projections show that hippocampal theta rhythm is an effective modulator of ACC and BLA theta oscillations that emerge during observational fear, and that the power of these oscillations bi-directionally tunes empathic fear.

## DISCUSSION

In this study, we successfully demonstrated that 5–7 Hz theta oscillations in the ACC and BLA in the right hemisphere are spatially, temporally, and quantitatively coupled with the emergence of observational fear. Neural oscillations have long been suggested as the mechanism by which the brain synchronizes distant brain areas for effective and organized brain functions.<sup>27–30</sup> However, the causal link between theta oscillations and specific brain functions has not been clearly established. We employed a closed-loop method employing a brief ChR2 stimulation that was shown to reliably disrupt sharp wave ripples in the hippocampus.<sup>20,21</sup> Our closed-loop experiment and bidi-

rectional modulation of theta activity through the hippocampus clearly demonstrate that theta oscillations at 5–7 Hz in the rACC-rBLA circuit are causally involved in observational fear.

Observational fear learning is a context-dependent fear conditioning where the US is provided through vicariously sharing the affective experience of the other under distress. Therefore, the levels of freezing on day 1 and 2 are expected to have a positive correlation.<sup>33</sup> In this view, it was unexpected that the significant effect of theta modulation on vicarious freezing on day 1 was not apparent on day 2 memory tests as shown in Figures 4, 5, and S3. On the other hand, experimental results of impaired freezing during conditioning but normal 24-h memory recall have been often reported.<sup>14,34,35</sup> Although the underlying mechanism is still unknown, at least in the current paradigm, these results may suggest the possibility that the encoding of memory may be separated mechanistically from the expression of vicarious fear.

We found that hippocampal theta rhythm is an important regulator of rACC-rBLA theta oscillations and observational fear. Optogenetic manipulations of septo-hippocampal GABAergic projections have been used and confirmed to selectively tune hippocampal theta oscillations.<sup>31,32</sup> To influence theta oscillations in broad hippocampal areas, including both dorsal and ventral subregions, which have distinct connectivity with the ACC and BLA,<sup>36,37</sup> we placed an optic fiber over the dorsal fornix that projects to the whole hippocampal complex.<sup>32,38,39</sup> The wide range of theta manipulations utilized in our study could be the main source of inconsistency relative to a recent report that local chemogenetic inhibition of either dorsal or ventral hippocampus does not alter naive observational fear behavior.<sup>12</sup>

Synchronous theta oscillations within the brain networks are known to be associated with communication among multiple areas for various cognitive and emotional functions.<sup>19,22,28,40–42</sup> Their causal relationship, however, has rarely been demonstrated. Within this context, the current study focuses on the specific moment of enhanced communication for empathic response through synchronized theta oscillations between the ACC, BLA, and hippocampus. At the moment, we do not know how hippocampal theta rhythms control the ACC-BLA rhythms. Future studies should address how multiple brain regions are simultaneously mobilized during observational fear, focusing on two things: First, it would be interesting to investigate the structural

**Figure 5. Hippocampal theta oscillations bi-directionally modulate ACC-BLA theta oscillations and observational fear**

- (A) AAV5-EF1 $\alpha$ -DIO-NpHR3.0-eYFP was injected into the MS of PV-Cre transgenic mice, and the dorsal fornix was illuminated with a yellow laser (top). eYFP expression in the MS, and eYFP expressing fibers imaged in the dorsal fornix (middle). LFP electrodes were implanted in the ACC, BLA, and hippocampus (bottom). Scale bars, 200  $\mu$ m.
- (B) Representative spectrograms for hippocampus, ACC, and BLA LFPs recorded during observational fear in the mouse of DIO-eYFP and DIO-NpHR.
- (C) Optogenetic inhibition of GABAergic MS inputs to the hippocampus significantly reduced freezing level during observational fear (left;  $F_{1, 11} = 10.87$ ,  $p < 0.01$ , two-way repeated measures ANOVA). Data are presented as means  $\pm$  SEM (error bars). \* $p < 0.05$ , \*\* $p < 0.01$ ; \*\*\* $p < 0.001$ ; post-hoc multiple comparison with Bonferroni correction. No statistical difference in 24-h contextual memory (right;  $p = 0.2093$ ,  $t(11) = 2.480$ ,  $t$  test).
- (D) Inhibition of MS GABAergic input to the hippocampus had no effect on freezing level during contextual fear conditioning (left;  $F_{1, 11} = 0.00289$ ,  $p = 0.958$ , two-way repeated measures ANOVA) or subsequent 24-h contextual memory (right;  $p = 0.817$ ,  $t(11) = 0.238$ ,  $t$  test).
- (E) AAV5-EF1 $\alpha$ -DIO-ChR2-eYFP was injected into the MS of PV-Cre transgenic mice, and the dorsal fornix was illuminated with a blue laser (left top). eYFP expression in the MS and eYFP-expressing fibers imaged in the dorsal fornix (left bottom). LFP electrodes were implanted in the ACC, BLA, and hippocampus (right). Scale bars, 200  $\mu$ m.
- (F) Optogenetic activation of GABAergic MS inputs to the hippocampus increased freezing level during observational fear conditioning (left;  $F_{1, 17} = 9.155$ ,  $p < 0.01$ , two-way repeated measures ANOVA). No statistical difference in 24-h contextual memory (right;  $p = 0.587$ ,  $t(17) = -0.554$ ). Data are presented as means  $\pm$  SEM (error bars). \* $p < 0.05$ , \*\* $p < 0.01$ ; \*\*\* $p < 0.001$ ; post-hoc multiple comparison with Bonferroni correction.
- (G) Pearson's correlation analysis of freezing behavior during observational fear versus averaged power changes in the 5–7 Hz frequency range.
- (H) Pearson's correlation analysis of freezing behavior during observational fear versus averaged phase locking value changes in the 5–7 Hz frequency range.

connections involved in the expression of observational fear. For example, the direct projections from the ventral hippocampus modulate anxiety behavior through its theta synchronization with mPFC and BLA in rodents.<sup>22,28</sup> The dorsal hippocampus also shows theta synchronization with the mPFC during working memory tasks.<sup>41</sup> The brain area, e.g., the midline thalamus, has reciprocal connections with the ACC/BLA and hippocampus.<sup>15,43</sup> There is also a possible indirect connection between the ACC, BLA, and hippocampus for theta communications during observational fear. Second, it would be interesting to investigate the molecular and cellular mechanisms underlying the generation and propagation of hippocampal theta oscillations to other brain areas. For example, enhanced and coordinated theta oscillations (although shown to be independent of the hippocampus) between the mPFC and BLA were implicated as mechanisms for recall and extinction of memory acquired after the direct foot-shock experience, and these oscillations are modulated by PV-interneurons in the respective brain area.<sup>19,40,42</sup> Meanwhile, somatostatin interneurons in the ACC are involved in regulation of observational fear rather than PV-interneurons.<sup>14</sup> Their involvement in regulation of theta oscillations in the ACC-BLA circuit could provide interesting insight into the mechanism of the theta rhythm lateralization to the right hemisphere.

Our results strongly indicate that hippocampal-dependent 5–7 Hz, type-2 theta synchronized oscillations in the rACC and rBLA specifically drive observational fear in mice. Considering the universality of observational fear across mammals, it is reasonable to suppose a similar neural signature critical for affective empathy may be found in humans and could be used to identify empathy dysfunction in humans with psychiatric disorders involving severe social deficits.

## STAR METHODS

Detailed methods are provided in the online version of this paper and include the following:

- **KEY RESOURCES TABLE**
- **RESOURCE AVAILABILITY**
  - Lead contact
  - Materials availability
  - Data and code availability
- **EXPERIMENTAL MODEL AND SUBJECT DETAILS**
  - Subjects
- **METHOD DETAILS**
  - Stereotaxic surgery and viral injection
  - Histology
  - Behavioral measurements
  - *In vivo* optogenetics
  - Local field potential recordings *in vivo* and analysis of theta oscillations
  - Closed-loop disruption of theta oscillations
- **QUANTIFICATION AND STATISTICAL ANALYSIS**

## SUPPLEMENTAL INFORMATION

Supplemental information can be found online at <https://doi.org/10.1016/j.neuron.2022.11.001>.

## ACKNOWLEDGEMENTS

This work was supported by grants from the Institute for Basic Science (IBS-R001-D1 and D2), Republic of Korea, and NIH/NINDS DP1 NS116783. This work was supported by “The 2022 Research Participation Grant on International Academic Project” from the National Academy of Sciences, Republic of Korea.

## AUTHOR CONTRIBUTIONS

Conceptualization, S.-W.K., M.K. and H.-S.S.; methodology, J.B., G.G. and C.-F.L.; programing, J.B.; investigation, S.-W.K., M.K., J.B., Y.Y., and D.-S.K.; writing – original draft, S.-W.K. and M.K.; writing – review & editing, M.K., J.B., J.H.L., and H.-S.S.; funding acquisition, J.H.L. and H.-S.S.; supervision, J.H.L. and H.-S.S.

## DECLARATION OF INTERESTS

J.H.L. is a founder, consultant, and board member of LVIS. H.-S.S. is a chief science officer of SL Bigen.

Received: April 25, 2022

Revised: September 22, 2022

Accepted: November 1, 2022

Published: December 1, 2022

## REFERENCES

1. Haaker, J., Yi, J., Petrovic, P., and Olsson, A. (2017). Endogenous opioids regulate social threat learning in humans. *Nat. Commun.* 8, 15495. <https://doi.org/10.1038/ncomms15495>.
2. Jeon, D., Kim, S., Chetana, M., Jo, D., Ruley, H.E., Lin, S.Y., Rabah, D., Kinet, J.P., and Shin, H.S. (2010). Observational fear learning involves affective pain system and Cav1.2 Ca<sup>2+</sup> channels in ACC. *Nat. Neurosci.* 13, 482–488. <https://doi.org/10.1038/nn.2504>.
3. Mineka, S., and Cook, M. (1993). Mechanisms involved in the observational conditioning of fear. *J. Exp. Psychol. Gen.* 122, 23–38. <https://doi.org/10.1037/0096-3445.122.1.23>.
4. Olsson, A., and Phelps, E.A. (2007). Social learning of fear. *Nat. Neurosci.* 10, 1095–1102. <https://doi.org/10.1038/nn1968>.
5. Kleberg, J.L., Selbing, I., Lundqvist, D., Hofvander, B., and Olsson, A. (2015). Spontaneous eye movements and trait empathy predict vicarious learning of fear. *Int. J. Psychophysiol.* 98, 577–583. <https://doi.org/10.1016/j.ijpsycho.2015.04.001>.
6. Olsson, A., McMahon, K., Papenberg, G., Zaki, J., Bolger, N., and Ochsner, K.N. (2016). Vicarious fear learning depends on empathic appraisals and trait empathy. *Psychol. Sci.* 27, 25–33. <https://doi.org/10.1177/0956797615604124>.
7. Chen, Q., Panksepp, J.B., and Lahvis, G.P. (2009). Empathy is moderated by genetic background in mice. *PLoS One* 4, e4387. <https://doi.org/10.1371/journal.pone.0004387>.
8. Choi, J., and Jeong, Y. (2017). Elevated emotional contagion in a mouse model of Alzheimer’s disease is associated with increased synchronization in the insula and amygdala. *Sci. Rep.* 7, 46262. <https://doi.org/10.1038/srep46262>.
9. Twining, R.C., Vantrease, J.E., Love, S., Padival, M., and Rosenkranz, J.A. (2017). An intra-amygdala circuit specifically regulates social fear learning. *Nat. Neurosci.* 20, 459–469. <https://doi.org/10.1038/nn.4481>.
10. Allsop, S.A., Wichmann, R., Mills, F., Burgos-Robles, A., Chang, C.J., Felix-Ortiz, A.C., Vienne, A., Beyeler, A., Izadmehr, E.M., Globet, G., et al. (2018). Corticoamygdala transfer of socially derived information gates observational learning. *Cell* 173, 1329–1342.e18. <https://doi.org/10.1016/j.cell.2018.04.004>.

11. Smith, M.L., Asada, N., and Malenka, R.C. (2021). Anterior cingulate inputs to nucleus accumbens control the social transfer of pain and analgesia. *Science* 371, 153–159. <https://doi.org/10.1126/science.abe3040>.
12. Terranova, J.I., Yokose, J., Osanai, H., Marks, W.D., Yamamoto, J., Ogawa, S.K., and Kitamura, T. (2022). Hippocampal-amygdala memory circuits govern experience-dependent observational fear. *Neuron* 110, 1416–1431.e13. <https://doi.org/10.1101/j.neuron.2022.01.019>.
13. Singer, T., Seymour, B., O'Doherty, J., Kaube, H., Dolan, R.J., and Frith, C.D. (2004). Empathy for pain involves the affective but not sensory components of pain. *Science* 303, 1157–1162. <https://doi.org/10.1126/science.1093535>.
14. Keum, S., Kim, A., Shin, J.J., Kim, J.H., Park, J., and Shin, H.S. (2018). A missense variant at the Nrnxn3 locus enhances empathy fear in the mouse. *Neuron* 98, 588–601.e5. <https://doi.org/10.1101/j.neuron.2018.03.041>.
15. Kim, S., Mátyás, F., Lee, S., Acsády, L., and Shin, H.S. (2012). Lateralization of observational fear learning at the cortical but not thalamic level in mice. *Proc. Natl. Acad. Sci. USA* 109, 15497–15501. <https://doi.org/10.1073/pnas.1213903109>.
16. Mátyás, F., Lee, J., Shin, H.S., and Acsády, L. (2014). The fear circuit of the mouse forebrain: connections between the mediodorsal thalamus, frontal cortices and basolateral amygdala. *Eur. J. Neurosci.* 39, 1810–1823. <https://doi.org/10.1111/ejn.12610>.
17. Burgos-Robles, A., Vidal-Gonzalez, I., and Quirk, G.J. (2009). Sustained conditioned responses in prelimbic prefrontal neurons are correlated with fear expression and extinction failure. *J. Neurosci.* 29, 8474–8482. <https://doi.org/10.1523/JNEUROSCI.0378-09.2009>.
18. Sierra-Mercado, D., Padilla-Coreano, N., and Quirk, G.J. (2011). Dissociable roles of prelimbic and infralimbic cortices, ventral hippocampus, and basolateral amygdala in the expression and extinction of conditioned fear. *Neuropharmacology* 56, 529–538. <https://doi.org/10.1038/npp.2010.184>.
19. Karalis, N., Dejean, C., Chaudun, F., Khoder, S., Rozeske, R.R., Wurtz, H., Bagur, S., Benchenane, K., Sirota, A., Courtin, J., and Herry, C. (2016). 4-Hz oscillations synchronize prefrontal-amygdala circuits during fear behavior. *Nat. Neurosci.* 19, 605–612. <https://doi.org/10.1038/nn.4251>.
20. Fernández-Ruiz, A., Oliva, A., Fermino de Oliveira, E., Rocha-Almeida, F., Tingley, D., and Buzsáki, G. (2019). Long-duration hippocampal sharp wave ripples improve memory. *Science* 364, 1082–1086. <https://doi.org/10.1126/science.aax0758>.
21. Oliva, A., Fernández-Ruiz, A., Leroy, F., and Siegelbaum, S.A. (2020). Hippocampal CA2 sharp-wave ripples reactivate and promote social memory. *Nature* 587, 264–269. <https://doi.org/10.1038/s41586-020-2758-y>.
22. Adhikari, A., Topiwala, M.A., and Gordon, J.A. (2010). Synchronized activity between the ventral hippocampus and the medial prefrontal cortex during anxiety. *Neuron* 65, 257–269. <https://doi.org/10.1101/j.neuron.2009.12.002>.
23. Buzsáki, G., and Moser, E.I. (2013). Memory, navigation and theta rhythm in the hippocampal-entorhinal system. *Nat. Neurosci.* 16, 130–138. <https://doi.org/10.1038/nn.3304>.
24. Danjo, T., Toyoizumi, T., and Fujisawa, S. (2018). Spatial representations of self and other in the hippocampus. *Science* 359, 213–218. <https://doi.org/10.1126/science.aoa3898>.
25. Seidenbecher, T., Laxmi, T.R., Stork, O., and Pape, H.C. (2003). Amygdalar and hippocampal theta rhythm synchronization during fear memory retrieval. *Science* 301, 846–850. <https://doi.org/10.1126/science.1085818>.
26. Tamura, M., Spellman, T.J., Rosen, A.M., Gogos, J.A., and Gordon, J.A. (2017). Hippocampal-prefrontal theta-gamma coupling during performance of a spatial working memory task. *Nat. Commun.* 8, 2182. <https://doi.org/10.1038/s41467-017-02108-9>.
27. Mague, S.D., Talbot, A., Blount, C., Walder-Christensen, K.K., Duffney, L.J., Adamson, E., Bey, A.L., Ndubuiwu, N., Thomas, G.E., Hughes, D.N., et al. (2022). Brain-wide electrical dynamics encode individual appetitive social behavior. *Neuron* 110, 1728–1741.e7. <https://doi.org/10.1101/j.neuron.2022.02.016>.
28. Padilla-Coreano, N., Bolkan, S.S., Pierce, G.M., Blackman, D.R., Hardin, W.D., Garcia-Garcia, A.L., Spellman, T.J., and Gordon, J.A. (2016). Direct ventral hippocampal-prefrontal input is required for anxiety-related neural activity and behavior. *Neuron* 89, 857–866. <https://doi.org/10.1101/j.neuron.2016.01.011>.
29. Popa, D., Duvarci, S., Popescu, A.T., Léna, C., and Paré, D. (2010). Coherent amygdalocortical theta promotes fear memory consolidation during paradoxical sleep. *Proc. Natl. Acad. Sci. USA.* 107, 6516–6519. <https://doi.org/10.1073/pnas.0913016107>.
30. Çalışkan, G., and Stork, O. (2019). Hippocampal network oscillations at the interplay between innate anxiety and learned fear. *Psychopharmacol. (Berl.)* 236, 321–338. <https://doi.org/10.1007/s00213-018-5109-z>.
31. Boyce, R., Glasgow, S.D., Williams, S., and Adamantidis, A. (2016). Causal evidence for the role of REM sleep theta rhythm in contextual memory consolidation. *Science* 352, 812–816. <https://doi.org/10.1126/science.aad5252>.
32. Gangadharan, G., Shin, J., Kim, S.W., Kim, A., Paydar, A., Kim, D.S., Miyazaki, T., Watanabe, M., Yanagawa, Y., Kim, J., et al. (2016). Medial septal GABAergic projection neurons promote object exploration behavior and type 2 theta rhythm. *Proc. Natl. Acad. Sci. USA.* 113, 6550–6555. <https://doi.org/10.1073/pnas.1605019113>.
33. Keum, S., Park, J., Kim, A., Park, J., Kim, K.K., Jeong, J., and Shin, H.S. (2016). Variability in empathetic fear response among 11 inbred strains of mice. *Genes Brain Behav.* 15, 231–242. <https://doi.org/10.1111/gbb.12278>.
34. Corcoran, K.A., and Quirk, G.J. (2007). Activity in prelimbic cortex is necessary for the expression of learned, but not innate, fears. *J. Neurosci.* 27, 840–844. <https://doi.org/10.1523/JNEUROSCI.5327-06.2007>.
35. Gidyk, D.C., McDonald, R.J., and Sutherland, R.J. (2021). Intact behavioral expression of contextual fear, context discrimination, and object discrimination memories acquired in the absence of the hippocampus. *J. Neurosci.* 41, 2437–2446. <https://doi.org/10.1523/JNEUROSCI.0546-20.2020>.
36. Bian, X.L., Qin, C., Cai, C.Y., Zhou, Y., Tao, Y., Lin, Y.H., Wu, H.Y., Chang, L., Luo, C.X., and Zhu, D.Y. (2019). Anterior cingulate cortex to ventral hippocampus circuit mediates contextual fear generalization. *J. Neurosci.* 39, 5728–5739. <https://doi.org/10.1523/JNEUROSCI.2739-18.2019>.
37. Rajasethupathy, P., Sankaran, S., Marshel, J.H., Kim, C.K., Ferenczi, E., Lee, S.Y., Berndt, A., Ramakrishnan, C., Jaffe, A., Lo, M., et al. (2015). Projections from neocortex mediate top-down control of memory retrieval. *Nature* 526, 653–659. <https://doi.org/10.1038/nature15389>.
38. Freund, T.F., and Antal, M. (1988). GABA-containing neurons in the septum control inhibitory interneurons in the hippocampus. *Nature* 336, 170–173. <https://doi.org/10.1038/336170a0>.
39. Senova, S., Fomenko, A., Gondard, E., and Lozano, A.M. (2020). Anatomy and function of the fornix in the context of its potential as a therapeutic target. *J. Neurol. Neurosurg. Psychiatry* 91, 547–559. <https://doi.org/10.1136/jnnp-2019-322375>.
40. Davis, P., Zaki, Y., Maguire, J., and Reijmers, L.G. (2017). Cellular and oscillatory substrates of fear extinction learning. *Nat. Neurosci.* 20, 1624–1633. <https://doi.org/10.1038/nn.4651>.
41. O'Neill, P.K., Gordon, J.A., and Sigurdsson, T. (2013). Theta oscillations in the medial prefrontal cortex are modulated by spatial working memory and synchronize with the hippocampus through its ventral subregion. *J. Neurosci.* 33, 14211–14224. <https://doi.org/10.1523/JNEUROSCI.2378-13.2013>.
42. Ozawa, M., Davis, P., Ni, J., Maguire, J., Papouin, T., and Reijmers, L. (2020). Experience-dependent resonance in amygdalo-cortical circuits

- supports fear memory retrieval following extinction. *Nat. Commun.* 11, 4358. <https://doi.org/10.1038/s41467-020-18199-w>.
43. Vertes, R.P., Linley, S.B., and Hoover, W.B. (2015). Limbic circuitry of the midline thalamus. *Neurosci. Biobehav. Rev.* 54, 89–107. <https://doi.org/10.1016/j.neubiorev.2015.01.014>.
44. Frankland, P.W., Bontempi, B., Talton, L.E., Kaczmarek, L., and Silva, A.J. (2004). The involvement of the anterior cingulate cortex in remote contextual fear memory. *Science* 304, 881–883. <https://doi.org/10.1126/science.1094804>.
45. Gramfort, A., Luessi, M., Larson, E., Engemann, D.A., Strohmeier, D., Brodbeck, C., Goj, R., Jas, M., Brooks, T., Parkkonen, L., Hämäläinen, et al. (2013). MEG and EEG data analysis with MNE-Python. *Front. Neurosci.* 7, 267. <https://doi.org/10.3389/fnins.2013.00267>.

## STAR★METHODS

## KEY RESOURCES TABLE

REAGENT or RESOURCE	SOURCE	IDENTIFIER
<b>Bacterial and virus strains</b>		
AAV5-CamKIIa-NpHR3.0-eYFP	UNC vector core	RRID: SCR_002448
AAV5-CamKIIa-eYFP	UNC vector core	RRID: SCR_002448
AAV5-EF1a-DIO-NpHR3.0-eYFP	UNC vector core	RRID: SCR_002448
AAV5-EF1a-DIO-ChR2-eYFP	UNC vector core	RRID: SCR_002448
AAV5-EF1a-DIO- eYFP	UNC vector core	RRID: SCR_002448
<b>Chemicals, peptides, and recombinant proteins</b>		
VECTASHIELD HardSet mounting medium with DAPI	Vector Laboratories	Cat# H-1500
<b>Experimental models: Organisms/strains</b>		
Mouse: PV-IRES-Cre: B6;129P2- <i>Pvalb</i> <sup>tm1(cre)Arbr</sup> /J	The Jackson Laboratory	JAX: 008069; RRID: IMSR_JAX:008069
Mouse: C57BL6/J	The Jackson Laboratory	JAX: 000664; RRID: IMSR_JAX:000664
<b>Software and algorithms</b>		
R Project for Statistical Computing	<a href="https://www.r-project.org/">https://www.r-project.org/</a>	RRID: SCR_001905
Python Programming Language	<a href="https://www.python.org/">https://www.python.org/</a>	RRID: SCR_008394
Open Ephys	<a href="https://open-ephys.org/">https://open-ephys.org/</a>	RRID: SCR_021624
FreezeFrame	Coulbourn	RRID: SCR_014429
NIS-Elements	Nikon	RRID: SCR_014329
Codes for EEG analysis	This manuscript	<a href="https://doi.org/10.5281/zenodo.7262445">https://doi.org/10.5281/zenodo.7262445</a>
mne library	<sup>18</sup>	<a href="https://github.com/mne-tools/mne-python.git">https://github.com/mne-tools/mne-python.git</a>
<b>Other</b>		
ZIF-Clip digital head-stages	Tucker-Davis Technology	Cat# ZD32
RHD 16-Channel Recording Headstages	Intan technologies	Cat# C3335
RZ2 processor system	Tucker-Davis Technology	Cat# RZ2
Open Ephys acquisition board	Open Ephys	N/A
Yellow laser (561nm)	Changchun New Industries Optoelectronics Technology Corp.	Cat# MGL-FN-561
Blue laser (450nm)	Changchun New Industries Optoelectronics Technology Corp.	Cat# MDL-III-450

## RESOURCE AVAILABILITY

## Lead contact

Further information and requests for resources and reagents should be directed to and will be fulfilled by the lead contact, Dr. Hee-Sup Shin ([shin@ibs.re.kr](mailto:shin@ibs.re.kr)).

## Materials availability

This study did not generate new, unique reagents. Commercially available reagents are indicated in the [key resources table](#).

## Data and code availability

- The datasets generated and/or analyzed in the current study are available from the [lead contact](#) upon reasonable request.
- The original codes have been deposited at Zenodo: <https://doi.org/10.5281/zenodo.7262445>. The DOI is listed in the [key resources table](#).

- Any additional information required to reanalyze the data reported in this paper is available from the [lead contact](#) upon request.

## EXPERIMENTAL MODEL AND SUBJECT DETAILS

### Subjects

Adult male C57BL/6J mice (10–16 wk of age; RRID:IMSR\_JAX:000664) were used for behavioral experiments in **Figures 1, 2, 3, and 4**, and **S1–S3**. Adult male Pvalb<sup>tm1(cre)Arbr</sup> (PV-Cre) mice (10–16 wk of age; RRID:IMSR\_JAX:008069), used for manipulating septo-hippocampal GABAergic projections in **Figures 5, S4, and S5**, were obtained from The Jackson Laboratory. Sample size for each experiment is described in the legend of figure. It should be noted that one mouse for Post-theta and two mice for On-theta were excluded from the LFP analysis. Due to the disconnected ACC electrodes in these mice, they were only used to test behavioral changes following BLA disruption since LFP signals could still be normally monitored in the BLA. Therefore, the sample sizes for the LFP analysis (**Figures S3C–S3F**; n = 7 for Post-theta, 5 for On-theta) and behavior analysis (**Figures S3G–S3H**; n = 8 for Post-theta, 7 for On-theta) are different in **Figure S3**. Mice were maintained under a 12/12-h light/dark cycle (lights on at 8:00 a.m.), with free access to food and water. Animal care and experimental procedures followed the guidelines of the Institutional Animal Care and Use Committee of the Institute for Basic Science.

### METHOD DETAILS

#### Stereotaxic surgery and viral injection

Mice were placed in an induction chamber (Vapormatic Ltd.) filled with a mixture of isoflurane (4%) and oxygen (delivered at 2 l/min) and anesthetized by intraperitoneal injection of a mixture of ketamine (120 mg/kg) and xylazine (10 mg/kg) in saline (0.015 ml/g). The head of each anesthetized mouse was fixed on a stereotaxic frame (Kopf Instruments), and a heating pad was used to ensure maintenance of core body temperature at 36°C. Cranial openings were made with dental drills, and virus solution was injected into the mouse brain using a Picospritzer III (Parker Hannifin Corp.). For optogenetic inhibition of ACC-BLA, BLA-ACC, and mPFC-BLA pathways, AAV5-CaMKIIα-NpHR3.0-eYFP was injected into the ACC (+1.0 anteroposterior, +0.3 or -0.3 mediolateral, and -1.2 dorsoventral from the bregma), BLA (-1.4 anteroposterior, +3.2 or -3.2 mediolateral, and -4.75 dorsoventral), and bilateral mPFC (+1.6 anteroposterior, ±0.3 mediolateral, and -2.6 dorsoventral), respectively. For closed-loop disruption of theta oscillations, 0.5 μl of AAV5-CaMKIIα-ChR2-eYFP was injected into either the right ACC (+1.0 anteroposterior, +0.3 mediolateral, and -1.7 dorsoventral), or the right BLA (-1.4 anteroposterior, +3.2 mediolateral, and -4.75 dorsoventral). For optogenetic stimulation of septo-hippocampal GABAergic fibers, 0.5 μl of a Cre-dependent AAV expressing AAV5-EF1α-DIO-NpHR3.0-eYFP or AAV5-EF1α-DIO-ChR2(H134R)-eYFP (Vector Core, University of North Carolina at Chapel Hill) was injected into the MS (+0.65 anteroposterior, 0.0 mediolateral, and -3.6 dorsoventral) of PV-Cre mice. AAVs expressing eYFP alone under control of the EF1α promoter (AAV5-EF1α-DIO-eYFP) were used as a non-targeting control virus.

#### Histology

Mice were anesthetized and transcardially perfused with 4% paraformaldehyde in phosphate-buffered saline (PBS). Brains were removed and post-fixed with the same solution, after which coronal sections were prepared at a thickness of 50 μm using a vibratome. The sites of viral expression and fiber implantation were verified by imaging sliced sections mounted with VECTASHIELD mounting media containing 4',6-diamidino-2-phenylindole (DAPI; Vector Laboratories). Images were acquired using a Nikon A1R confocal microscope and NIS imaging software.

#### Behavioral measurements

The observational fear behavioral task was carried out according to procedures described previously.<sup>2</sup> Briefly, the apparatus for the observational fear task, prepared by modification of a passive avoidance cage (Coulbourn Instruments, Whitehall, PA, USA), consisted of two identical chambers (18 × 17.5 × 38 cm each) containing a transparent Plexiglas partition in the middle and a stainless-steel rod floor (5-mm diameter rods, spaced 1 cm apart). Sounds and odors could be transmitted between the chambers under the rod floor. For observational fear conditioning, mice (observer and demonstrator) were individually placed in the apparatus chambers for 5 min, after which a 2-s foot shock (1 mA) was delivered every 10 s for 4 min to one of the mice (demonstrator) via a computer-controlled animal shocker (Coulbourn Instruments). Contextual-dependent observational fear memory was assessed by placing the observer mouse alone back in the training context 24 h after training and measuring freezing behavior for 4 min. In all experiments, observer and demonstrator mice were non-siblings and non-cagemates. Fear responses were recorded and analyzed using Freeze-frame (V3.32) and Freezeview (Coulbourn Instruments) software. The SMP (significant motion pixels) algorithm in Freezeframe software was employed for automated analysis of activity and fear responses. Motionless bouts lasting more than 1 s were considered freezing events, and an SMP threshold value of 10 was used for all subjects.

A modified observational fear protocol was used in electrophysiological recordings with tetrodes to enhance separation of freezing responses and shock responses. In the modified protocol, mice were habituated in the chamber for 3 min, and 21 electric foot shocks were delivered to the demonstrator at pseudo-random intervals ranging from 13 s to 23 s with an average of 18 s. Times of freezing

onsets and offsets were identified manually by a frame-by-frame comparison of mouse movements in videos recorded at ~15 fps (~66.7-ms frame intervals, variable frame rate).

Contextual classical fear conditioning was performed as previously described with minor modifications.<sup>44</sup> On conditioning day, animals were subjected to three foot-shocks for **Figures 1** and **5** (2-s shocks, 0.8 mA, 1-min interval) or five shocks for **Figure S2E**(1-s shocks, 0.6 mA, pseud-random intervals with an average 99 s of intervals). After 24 h, mice were returned to the same context for 5 min for contextual memory recall. Freezing behavior, defined as a complete lack of movement (except for respiration) for longer than 1 s, was analyzed using Freezeframe software.

### **In vivo optogenetics**

Four to five weeks after virus injection, a fiber optic cannula (200  $\mu$ m core, 0.39 numerical aperture; Thorlabs) was implanted in i) the bilateral BLA (-1.4 anteroposterior,  $\pm$ 0.32 mediolateral, and -4.25 dorsoventral), for optogenetic inhibition of ACC-BLA projections; ii) the right ACC (+0.8 anteroposterior, +0.32 mediolateral, and +0.7 dorsoventral), for inhibition of BLA-ACC projections; and iii) the bilateral BLA (-1.4 anteroposterior,  $\pm$ 0.32 mediolateral, and -4.25 dorsoventral), for inhibition of mPFC-BLA projections. For optogenetic inhibition or activation of MS GABAergic projections to the hippocampus (MS<sup>GABA</sup>-Hipp), a fiber optic cannula (200  $\mu$ m core, 0.39 numerical aperture; Thorlabs) was implanted in the dorsal fornix (-0.3 anteroposterior, 0 mediolateral, and -2.25 dorsoventral). Mice were allowed to recover in individual housing for 1 to 2 wk before behavioral assays. One day before observational fear conditioning or contextual fear conditioning, fiber-implanted observer mice, with fiber optics coupled through zirconia sleeves, were additionally habituated to the chamber. Reciprocal excitatory connections between the right ACC and BLA or septo-hippocampal GABAergic projections were optogenetically inhibited during observational fear conditioning or contextual fear conditioning using a yellow laser (561 nm DPSS laser; CNI), with the power density adjusted to ~150 mW/mm<sup>2</sup> at the tip of the optic fibers (PM100D; Thorlabs). Laser illumination was initiated after a baseline period (5 min for observational fear conditioning; 3 min for contextual fear conditioning) and delivered continuously throughout the conditioning period (4 min for observational fear conditioning; 3 min for contextual fear conditioning). Optogenetic activation of septo-hippocampal GABAergic projections was achieved using a blue laser (445 nm DPSS laser; CNI) with a power density of 150 mW/mm<sup>2</sup> (MDL-III-450; 240 s duration, 20 Hz, 5 ms pulse width; Changchun New Industries Optogenetics Technology Corp.).

### **Local field potential recordings *in vivo* and analysis of theta oscillations**

#### **Data acquisition**

*In vivo* LFP recordings were performed as described previously.<sup>2,32</sup> For comparisons of left and right hemispheres, arrays of 8 tetrodes were implanted in the ACC (+1.0 anteroposterior, +0.3 or -0.3 mediolateral, and -1.7 dorsoventral from the bregma) or BLA (-1.5 anteroposterior, +3.1 mediolateral, and -4.8 dorsoventral from the bregma). For closed-loop disruption of the ACC theta activity, an array of 8 tetrodes and an optic fiber (200  $\mu$ m core, 0.39 numerical aperture) was placed over the rACC (+1.0 anteroposterior, +0.3 mediolateral, and -1.7 dorsoventral, and an array of 16 tetrodes was implanted in the rBLA (-1.5 anteroposterior, +3.1 mediolateral, and -4.8 dorsoventral). For closed-loop disruption of the BLA theta activity, a tungsten electrode (0.002" diameter; A-M Systems) and an optic fiber (200  $\mu$ m core, 0.39 numerical aperture) was placed over the rBLA (-1.5 anteroposterior, +3.1 mediolateral, and -4.8 dorsoventral), and a tungsten electrode was implanted in the rACC (+1.0 anteroposterior, +0.3 mediolateral, and -1.7 dorsoventral). For optogenetic manipulation of septo-hippocampal GABAergic projections, an optic fiber (200  $\mu$ m core, 0.39 numerical aperture) was implanted in the dorsal fornix (-0.3 anteroposterior, 0 mediolateral, and -2.25 dorsoventral), and tungsten electrodes (0.005 inch, 100 K $\Omega$ ) were positioned unilaterally in the right hemisphere ACC (+1.0 anteroposterior, +0.3 mediolateral, and -1.2 dorsoventral), BLA (-1.4 anteroposterior, +3.2 mediolateral, and -4.7 dorsoventral), or hippocampal fissure (-1.4 anteroposterior, +1.2 mediolateral, and -1.8 dorsoventral), with grounding over the cerebellum. Electrophysiological recordings were performed using ZIF-Clip digital head-stages (Tucker-Davis Technology) or RHD 16-Channel Recording Headstages (Intan Technologies) connected to a RZ2 processor system (Tucker-Davis Technology) or an Open-Ephys board (<http://open-ephys.org>; RRID: SCR\_021624). Signals were acquired at 24 kHz (RZ2 processor) or 30 kHz (Open-Ephys board), and bandpass-filtered at 0.1-100 Hz.

#### **Closed-loop disruption of theta oscillations**

Theta events in the rACC were detected online using a custom-built, real-time Gizmo module in Synapse software (Tucker-Davis Technology), and theta events in the rBLA were detected using a custom-built Open-Ephys plugin. The power of the LFP signal at 4-8 Hz was estimated and divided by the broad-band spectral power. The calculated theta ratio was continuously monitored and compared with a threshold level, which was manually adjusted for each subject before the start of behavioral experiments. The theta epoch was defined as an LFP segment with a theta ratio larger than the threshold value for more than 200 ms. The number of online detected theta events during habituation was not different between groups (ACC closed-loop,  $P = 0.7571$ ,  $t(13) = 0.31595$ ; BLA closed-loop,  $P = 0.8359$ ,  $t(13) = 0.21138$ , t-test). Once a theta event was detected, a short (10-ms) light pulse (445 nm, ACC; 473 nm, BLA) was delivered. In the On-theta group, the light pulse was turned on 200 ms after threshold crossing. In the Post-theta group, ChR2 stimulation was delivered 500-1000 ms after offset of the theta epoch.

#### **Data analysis**

LFP signals were downsampled to 1 kHz and filtered at 1-40 Hz for further analysis. Large-amplitude ChR2 artifacts recorded in the closed-loop theta disruption experiment were removed by discarding data segments -10 to 50 ms from laser onset and replaced by

cubic spline interpolation values. Spectral power around freezing epochs was estimated by time-frequency analysis using Morlet wavelets, with a center frequency of 2 to 20 Hz (in 0.2-Hz steps), and a length of five cycles. The estimated power was normalized to the total power at each time point. Then, for each subject, the normalized power was weighted by the duration of freezing and averaged over freezing epochs. Freezing-related changes were investigated by converting the weighted average power in each frequency into z-scores using -1.5 to -1 s from the onset of freezing as a baseline. The same baseline was used for z-score calculation of freezing-offset responses.

The phase value at each time and frequency was extracted using complex Morlet wavelets with a center frequency of 2 to 20 Hz (in 0.2-Hz steps), and a length of five cycles. The phase-locking value (PLV) over time was calculated for each freezing epoch and each frequency with a 5-cycle window size. For each subject, the calculated phase-locking value was then weighted by the duration of freezing and averaged over freezing epochs. Freezing-related changes were investigated by converting the weighted average PLV in each frequency into z-scores using -1.5 to -1 s from the onset of freezing as a baseline.

The effects of optogenetic manipulation of septo-hippocampal GABAergic projections on theta band activity in the ACC and BLA were analyzed from theta segments (4–12 Hz) identified in the right ACC. ACC theta epochs longer than 1 s were manually selected during the habituation period and inter-shock period during observational fear conditioning. The corresponding time segments from the BLA and hippocampus were analyzed together. Power spectral density was calculated by Welch's method, using a 1-s Hann window with 50% overlap. Phase-locking value (PLV) over time was calculated using Morlet wavelets with a length of five cycles. Changes in power or phase synchrony at 5–7 Hz were compared by calculating the ratio of the mean power spectral density or PLV at 5–7 Hz during the observational fear session to that during the habituation session. Data were analyzed using custom scripts for Python (RRID: SCR\_008394) and R (RRID: SCR\_001905).

#### QUANTIFICATION AND STATISTICAL ANALYSIS

Spectral analyses were performed using Python with mne library.<sup>45</sup> All statistical analyses were performed using R (RRID: SCR\_001905). Exact values of n and what n represents, the number of animals for each experiment, are indicated in the corresponding figure legends and Table S1. Normality was tested using Shapiro-Wilk test. The level of freezing during the observational fear and contextual fear conditioning were analyzed using post-hoc multiple comparison with Bonferroni correction after two-way repeated measures ANOVA on the conditioning day, and unpaired t-test on the 24-h memory recall. Averaged z-scores from onset, t = 0 to t = 1 s were used for the analyses of relative LFP power changes with t-test (one-sample, paired, and unpaired) and one-way repeated measures ANOVA for each purpose. Pearson's correlations between the level of freezing and change of power, or between the level of freezing and phase locking value at the range of 5–7 Hz. Data are presented as mean ± S.E.M., and P values < 0.05 were considered significant (\*P < 0.05, \*\*P < 0.01, \*\*\*P < 0.001).